

Automated Lane Merging via Game Theory and Branch Model Predictive Control

Luyao Zhang¹, Shaohang Han² and Sergio Grammatico¹

Abstract—We propose an integrated behavior and motion planning framework for the automated lane-merging problem. The behavior planner combines search-based planning with game theory to model the interaction between vehicles and select multi-vehicle trajectories. Inspired by human drivers, we model the lane-merging problem as a gap selection process. To overcome the challenge of multi-modal driving behavior exhibited by the surrounding vehicles, we formulate the trajectory selection as a matrix game and compute some equilibrium solutions. In practice, however, the surrounding vehicles might deviate from the computed equilibrium trajectories. Thus, we introduce a branch model predictive control (BMPC) framework to account for the uncertain behavior modes of the surrounding vehicles. A tailored numerical solver is developed to enhance computational efficiency by leveraging the tree structure inherent in BMPC. Finally, we validate our proposed integrated planner using real traffic data and demonstrate its effectiveness in handling interactions in dense traffic scenarios.

Index Terms—Behavior planning, game theory, trajectory tree, model predictive control, lane merging.

I. INTRODUCTION

THE last two decades have seen prosperous progress in autonomous driving technology. Nevertheless, navigating in highly interactive environments is still challenging for automated vehicles. One of the most demanding scenarios is the forced lane merging, where an automated vehicle needs to find a suitable gap and understand whether the surrounding vehicles are willing to yield or not. Traditional methods typically adopt a hierarchical structure where motion prediction and planning are decoupled [1], [2]. Consequently, these methods might be overly conservative since they often overlook the mutual interactions between the ego vehicle and the surrounding ones. Although recently developed learning-based approaches [3], [4] consider such interactions, their reliance on large amounts of data and the lack of interpretability pose both theoretical and practical challenges in safety-critical applications, such as autonomous driving. The Partially Observable Markov Decision Process (POMDP) is a widely recognized interaction-aware method, providing a robust mathematical framework for handling incomplete information [5]. In the context of autonomous driving, such incomplete information typically involves the unknown intentions of the surrounding vehicles [5]–[7]. In POMDPs, probabilistic generative models are used to simulate the reactive behavior of the surrounding

vehicles, and these models are parameterized to encode various driving intentions. While POMDPs provide rigorous models, their application in dense traffic scenarios remains a challenge due to computational constraints and poor scalability.

As an approximation of the POMDP framework, the multiple policy decision-making (MPDM) [8] and its extension EPSILON [9] have demonstrated promising results in generating practically reasonable trajectories while remaining computationally efficient. These approaches involve conducting interactive multi-vehicle forward simulations based on semantic-level policies, followed by a trajectory evaluation stage to select the optimal trajectory using handcrafted criteria. Unfortunately, whenever the surrounding vehicles have potentially diverse behavior modes, the rule-based trajectory evaluation in EPSILON might result in overly aggressive or overly conservative trajectories. Additionally, although the open-loop planning strategy in EPSILON is computationally efficient, it sacrifices the advantages of active information gathering in the original POMDP approach [10, Chapter 4.2.7].

Branch model predictive control (BMPC) [11], also known as contingency planning [12], [13] or trajectory tree motion planning (TTMP) [14], [15], are employed to deal with the multi-modal behavior exhibited by the surrounding vehicles. Conventional robust motion planners aim to generate one single smooth trajectory that is collision-free for all behavior modes [16], [17]. Unlike these conventional planners, which are prone to generate overly conservative trajectories, the BMPC approach involves constructing a trajectory tree with multiple branches. Each branch represents a potential future scenario, capturing various behavior modes. It is worth noting that only the shared nodes in the tree are required to satisfy the safety requirements across all possible scenarios, resulting in less conservative control inputs. Interestingly, BMPC methods share some similarities with POMDPs, particularly in terms of their tree structure. In POMDPs, the state and action space are typically discrete, while the BMPC approach assumes that only the unobservable intentions of the surrounding vehicles are discrete. Therefore, the BMPC problem can be cast as a stochastic optimal control problem, which can be solved by gradient-based optimization solvers [14], [15].

Similar to POMDPs and BMPC, game theory is another powerful mathematical framework that captures the mutual influence among multiple players. In both POMDPs and BMPC, surrounding vehicles are controlled by predefined prediction models without associated objective functions. In contrast, each player in a game has its individual cost function, which is dependent not only on its own action but also on the actions of other players, and the goal of each player is to optimize

*This work is partially supported by NWO under project AMADeUS.

Luyao Zhang and Sergio Grammatico are with the Delft Center for Systems and Control, TU Delft, The Netherlands. {l.zhang-7, s.grammatico}@tudelft.nl

²Shaohang Han is with the Department of Cognitive Robotics, TU Delft, The Netherlands. shaohang.han@outlook.com

its individual objective function. Previous research has extensively explored equilibrium solutions for autonomous driving. Some studies have focused on jointly planning trajectories for all vehicles by seeking a Nash equilibrium [18], [19]. However, these methods can only find a local equilibrium, and the quality of the solution might heavily depend on the initial guess. In contrast, other approaches utilize semantic-level actions as strategies to leverage domain knowledge of the lane-merging scenario. Among them, some studies investigate the Stackelberg equilibrium with a leader-follower game structure [20], [21]; however, determining the relative role of the leader or follower might be difficult in practice [20]. In contrast to the leader-follower structure, a Nash game treats all agents equally [18]. A representative method based on Nash games is proposed in [22], but it lacks validation in either a high-fidelity simulator or a real traffic dataset.

Contribution: We propose a novel interaction-aware planning framework that integrates game theory, interactive trajectory generation, and BMPC. Our contributions are summarized as follows:

- (i) We consider the multi-modality problem from a game-theoretic perspective by modeling the interaction between vehicles as a dynamic game (Section III).
- (ii) We introduce a matrix game as an approximation of the original dynamic game (Section IV). To make the algorithm practical and efficient, we approximate the action space of the dynamic game by using semantic-level actions (Section IV-A) and forward simulating the multi-vehicle system (Section IV-B). Moreover, we account for the unknown cost functions by incorporating the belief about the behavior mode (Section IV-C).
- (iii) Since our method can compute multiple equilibria, we propose an approach for equilibrium selection (Section IV-C).

A preliminary version of this work was presented in [23]. In this extended paper, we present the following additional contributions:

- (iv) We consider the multi-modality problem not only in the behavior planner but also in the motion planner. To achieve this, we develop a BMPC framework and propose a method for initializing the trajectory tree based on our game-theoretic behavior planner (Section V). Additionally, we implement a customized numerical solver that exploits the problem structure to achieve real-time performance (Section VI-B).
- (v) To validate the effectiveness of the proposed game-theoretic planning framework, we conduct extensive numerical simulations on real-traffic data, specifically, on the INTERACTION dataset [24] (Section VI). Moreover, we compare our newly proposed planner with our previous one and other baseline methods.

II. RELATED WORKS

A. POMDP

Extensive research has focused on applying POMDP to address the issue of the intentions of the surrounding vehicles being unknown. One line of research is dedicated to approximat-

ing original POMDP problems and enhancing computational efficiency. Online solvers, such as POMCP [25], POMCPOW [26], and DESOPT [27], employ sampling techniques to estimate the action-value function. Other heuristic approximations of POMDP have also been introduced for specific autonomous driving applications to facilitate the search process. Hubmann et al. [6] combines the Monte Carlo sampling algorithm with an A* roll-out heuristic for fast convergence. Their planner can generate interactive policies for lane-merging scenarios. Fischer et al. [28] proposes an interactive lane-merging planner that utilizes trained policies to guide online belief planning. In [7], [29], the authors investigate the unsignalized intersection scenario and elaborately design the state and action space to achieve a low-dimensional problem that is solvable in practice. The reader can refer to [5] for a comprehensive survey on POMDP and its applications in robotics.

B. Branch Model Predictive Control

BMPC is categorized as an optimization-based method. In autonomous driving applications, BMPC is used to account for the uncertain behavior modes of the surrounding vehicles. Methods for BMPC vary in their approaches to modeling the surrounding vehicles. In [12], [30], [31], the motion of the surrounding vehicles is determined by the predicted multi-modal trajectories produced by the prediction module. These methods assume that both the future trajectory of each surrounding vehicle and the probability associated with each tree branch are fixed; this implies that the ego vehicle cannot affect the motion of the surrounding vehicle. To further exploit the benefit of the interaction, Chen et al. [11] and Wang et al. [14] employ the predefined interactive motion models and construct the trajectory trees with multiple branches; however, the probability linked to each branch depends only on the current joint state, rather than the observed historical trajectories. Consequently, their formulations lack the incorporation of belief updates. For active information gathering, the authors in [13], [15] present a complete BMPC framework that includes the belief update.

C. Game-Theoretic Planning

Game-theoretic planning has recently become popular due to its capability of modeling the complex interactions among multiple players. Many research efforts have been devoted to developing efficient equilibrium seeking algorithms [18], [19], [32]. The game-theoretic planners in these references break the traditional predict-and-plan framework by jointly planning trajectories for all vehicles. In these methods, the objective functions of the surrounding vehicles encode driving behavior. However, in practice, these objective functions are unknown to the ego vehicle. To identify them, various approaches have been proposed, including those based on particle filtering [33], optimality conditions [34], and differentiable optimization [19]. In contrast to joint motion planning, alternative approaches focus on the decision-making problem, where strategies are represented by discrete semantic-level decisions. In [20], the authors design the strategies of the ego vehicle as motion primitives and use a leader-follower game

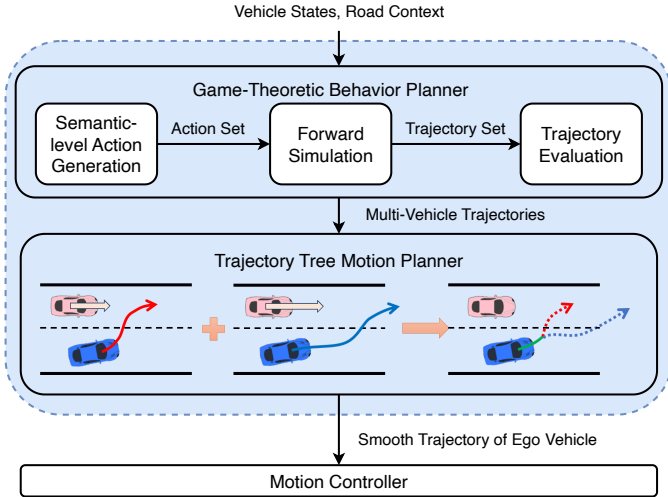


Fig. 1. Structure of the proposed game-theoretic planner. The behavior planner outputs the multi-vehicle trajectories which reflect the semantic-level actions of the relevant vehicles. In the trajectory tree, the shared trajectory is shown in green, and the contingency trajectories are represented by the dashed curves.

to model the behavior of the surrounding vehicles. Zhang et al. [35] and Wei et al. [21] represent the strategy of the ego vehicle as the waiting time before merging and seek a Stackelberg equilibrium. In the context of Stackelberg games, while most methods assume the ego vehicle to be the leader, the underlying rationale behind this choice is not always clear. In addition to Nash and Stackelberg games, other approaches utilize level- k reasoning to model human driving behavior [36], [37]. However, the computational burden of this framework is substantial due to the necessity of modeling the depth of human thinking [38].

III. PROBLEM SETTING

We consider a mixed-traffic scenario where an automated vehicle (ego vehicle) interacts with the surrounding vehicles, as shown in Figure 2a. The ego vehicle aims at executing a lane change as it is approaching the end of the current lane. To avoid being blocked, its decision-making system must account for various factors, including the merging gap, the timing for lane changing, and the diverse behavior modes of the surrounding vehicles. For example, in Figure 2a, the ego vehicle can select to merge ahead of or after the SV1. If the SV1 yields, then the gap enlarges and the ego vehicle merges ahead of the SV1; otherwise, if the gap is not sufficiently wide, the ego vehicle might slow down and merge after the SV1.

A. General Structure of the Planner

We propose a game-theoretic planning framework, as illustrated in Figure 1. Unlike traditional behavior planners that usually require a motion predictor as an upstream module, our approach combines motion prediction and behavior planning. The proposed game-theoretic behavior planner comprises three core modules: semantic-level action generation, forward simulation, and trajectory evaluation. We first enumerate the possible semantic-level decision sequences of the considered

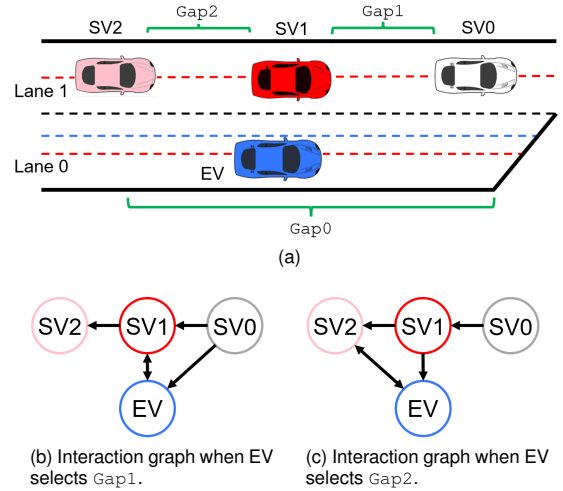


Fig. 2. (a): The forced lane-merging problem: three gaps are available for the ego vehicle to choose from: Gap0, Gap1 and Gap2. The dashed red lines represent the centerlines of the lanes, and the dashed blue line represents the probing line. EV stands for the ego vehicle (blue), while SV0, SV1, and SV2 denote the surrounding vehicles. (b)-(c): Illustrate the interaction graphs when EV selects Gap1 and Gap2, respectively. The single-headed arrow indicates one-way influence, while double-headed arrows denote mutual interaction.

vehicles. For the ego vehicle, a semantic-level decision typically involves making a lane change, accelerating or decelerating. Then, we create the action pairs by combining the decision sequences of the ego vehicle and surrounding vehicles. For each action pair, the forward simulator generates the multi-vehicle trajectories. The costs of these trajectories are computed by the trajectory evaluator. Next, we construct a matrix game and seek an equilibrium. Finally, the trajectory evaluator selects the action pair associated with the equilibrium and outputs the corresponding multi-vehicle trajectories.

We employ an additional motion planner to enhance trajectory smoothness. Furthermore, we develop a BMPC planner to handle the multi-modal behavior exhibited by the surrounding vehicles. To ensure safety, the simulated trajectories of the surrounding vehicles are used to impose dynamic collision avoidance constraints.

B. Dynamic Game-Theoretic Setting

We model the interaction between vehicles using a finite horizon dynamic game with N vehicles. For each vehicle i , we consider the discrete-time dynamics

$$x_{t+1}^i = f(x_t^i, u_t^i), \quad (1)$$

where $t \in [0, T-1] := \{0, \dots, T-1\}$, $x_t^i \in \mathbb{R}^n$ and $u_t^i \in \mathbb{R}^m$ denote the state and control input vectors at time step t . For notational simplicity, the notation without a superscript refers to all vehicles, while the notation without t refers to all time steps. For instance, x_t represents the states of all vehicles at time step t , while x^i denotes the state trajectory of vehicle i . Moreover, x^{-i} and u^{-i} are the stacked state and control input vectors of all vehicles except vehicle i , respectively. In an open-loop dynamic game, each vehicle selects a control input sequence to optimize its individual objective function. Thus,

we formulate the N interdependent optimization problems as follows:

$$\begin{cases} \min_{u^i} & J^i(\mathbf{x}, u^i, \mathbf{u}^{-i}) & (2a) \\ \text{s.t.} & x_{t+1}^i = f(x_t^i, u_t^i), \quad \forall t \in [0, T-1], & (2b) \\ & u_t^i \in \mathcal{U}, \quad \forall t \in [0, T-1], & (2c) \end{cases}$$

where $\mathcal{U} \subseteq \mathbb{R}^m$ denotes the feasible control input set, T is the horizon and the cost function J^i depends on both the joint state trajectory and the control input vectors for each vehicle. The solution to (2) is a Nash equilibrium, where no vehicle can further reduce its cost by unilaterally changing its control input sequence. Unfortunately, directly solving (2) is challenging due to the nonconvex cost function (2a) and the nonlinear dynamics (2b). Consequently, if the initial guess is relatively far from an equilibrium, the solution is likely to get stuck in an undesirable point. To mitigate the aforementioned issues, we use the search-based method, which can explore the solution space more extensively. Specifically, we first discretize the control input space in (2) and then formulate a matrix game with discrete action space. A matrix game can be defined by a tuple (\mathcal{N}, Π, J) , where \mathcal{N} is the set of players, $\Pi = \times_{i \in \mathcal{N}} \Pi^i$ is the joint action space, and $J = \{J^i\}_{i \in \mathcal{N}}$ are the cost functions. Next, we introduce the three ingredients of the matrix game: players, actions, and cost functions.

1) *Players*: In principle, we need to consider both the ego vehicle and all relevant surrounding vehicles as players. This choice accounts for the interaction between each pair of vehicles but leads to a complex multi-player matrix game. To simplify the matrix game, we make the following assumptions based on the inherent properties of the lane-merging problem.

Assumption 1. *The surrounding vehicles maintain their lanes and move longitudinally [20, Section 2], [21, Section 3].*

Figures 2b and 2c illustrate the simplified interaction relations. Specifically, we focus on the mutual interaction between the ego vehicle (EV) and one single surrounding vehicle, denoted as the interacting vehicle (IV). All other vehicle interactions are considered unidirectional. For example, in Figure 2b, the EV does not influence the vehicle (SV0) ahead of the IV (SV1), and the SV2 may be affected by the IV (SV1) but does not influence the EV. To sum up, we make the following assumption:

Assumption 2. *Within the planning cycle, the ego vehicle mutually interacts with at most one surrounding vehicle (interacting vehicle), as illustrated in Figure 2b and 2c.*

Next, inspired by RSS [39], we assume that the SVs with one-way interactions always take action to avoid colliding with the lead vehicle. Combining this with Assumption 2, we can treat the SVs as a vehicle group (VG). In the group, the IV owns multiple semantic-level actions, while the remaining SVs exhibit car-following behavior. To sum up, we consider the EV and the group of SVs (VG) as two players, $\mathcal{N} := \{\text{EV}, \text{VG}\}$.

2) *Actions*: One straightforward choice for the action is the control input sequence of each player, which can be obtained by discretizing the control input space. However, this approach results in large action sets and a large-scale matrix

game that is potentially challenging to solve. Moreover, if we independently sample the control input space for each player, the potential interaction between players would be ignored, and the resulting trajectories might not be realistic. Inspired by human drivers, we instead represent the action of player $i \in \mathcal{N}$ by a semantic-level decision sequence, denoted as $\pi^i := \{\pi_0^i, \dots, \pi_k^i, \dots, \pi_{H-1}^i\}$, where H is the decision horizon. We provide more design details on the decision sets and the method for enumerating all possible decision sequences later in Section IV-A.

3) *Objective functions*: For each action pair, the forward simulator (Section IV-B) generates the corresponding multi-vehicle trajectories, and then we compute the costs of the trajectories. The cost function J^i of vehicle i evaluates the corresponding trajectory based on user-defined metrics, such as safety, efficiency, comfort, and navigation. We consider the SVs as a vehicle group by calculating the total cost as $J^{\text{VG}} := \sum_{i \neq \text{EV}} J^i$. More technical details are provided in Section IV-C.

The matrix game is represented by a table, where each entry represents a cost pair $(J_{ij}^{\text{VG}}, J_{ij}^{\text{EV}})$ received by the VG and the EV after performing their respective actions, π_i^{VG} and π_j^{EV} (see [23]). In the table, we seek an equilibrium of the following types:

Definition 1. *(Pure-strategy Nash equilibrium). A pure-strategy Nash equilibrium is a set of players' actions, $\{\pi^{i*}\}_{i \in \mathcal{N}}$ such that, for each player i , it holds that*

$$J^i(\pi^{i*}, \pi^{-i*}) \leq \inf_{s^i \in \Pi^i} J^i(s^i, \pi^{-i*}),$$

where π^{-i} represents the set of actions taken by all players except player i .

Definition 2. *(Stackelberg equilibrium). A Stackelberg equilibrium is a pair $\{\pi^{L*}, \pi^{F*}(\cdot)\}$ such that*

$$\begin{aligned} \pi^{L*} &= \arg \min_{\pi^L \in \Pi^L} J^L(\pi^L, \pi^{F*}(\pi^L)), \\ \pi^{F*}(\pi^L) &= \arg \min_{\pi^F \in \Pi^F} J^F(\pi^L, \pi^F), \end{aligned}$$

where the superscripts, L and F , represent the leader and the follower of the game, respectively.

In a Stackelberg game, the idea is that the leader can take the action first, and then the follower plays the best response action [40]. The leader and follower roles are not always fixed on the road. In other words, the EV can switch between being the leader and the follower [41]. Thus, we can consider two Stackelberg equilibria: one with the EV as the leader and the other with the EV as the follower.

The proposed matrix game can be viewed as a discrete approximation of (2). Compared with solving the origin problem, the solution to the matrix game is easy to compute, e.g. by enumeration. Moreover, owing to the context-aware action generation and interactive forward simulation, the problem size is moderate.

IV. GAME-THEORETIC BEHAVIOR PLANNING

A. Semantic-Level Action Generation

1) *Actions of Ego Vehicle*: In the lane-merging problem, the semantic-level decision involves selecting a gap and determining a desired lateral position. For example, in Figure 2a, the EV has three potential gaps to choose from. To reach the target gap, the EV needs to perform a sequence of lateral decisions. The common lateral decisions are lane changing and lane keeping. Additionally, we introduce one additional intermediate lane, represented by the dashed blue line in Figure 2a, to enable a probing decision. This allows the EV to gather information and negotiate with the SVs. Overall, the complete lateral decision set can be defined as:

$$D^{\text{lat}} := \{\text{LaneKeep}, \text{LeftChange}, \text{LeftProbe}\}.$$

The semantic-level decision at decision step k is denoted by an action pair $\pi_k^{\text{EV}} := (g_k, d_k^{\text{lat}})$, where $g_k \in \{\text{Gap0}, \text{Gap1}, \text{Gap2}\}$ and $d_k^{\text{lat}} \in D^{\text{lat}}(g_k)$. We note that the lateral decision set is conditioned on the gap selection, which reduces the number of action pairs. For example, if the EV chooses Gap0, then the only available lateral action is to keep the current lane.

Next, in line with [9], we construct a decision tree to enumerate all possible decision sequences. Each node in the tree represents a decision pair. The decision tree is rooted in the decision selected in the last planning cycle and branches out at each decision step. Due to the exponential growth of the number of decision sequences with the depth of the tree, it is necessary to prune the decision tree to limit computational complexity. By using semantic-level decisions, we can design some rules to prune the tree. For instance, we can restrict the number of decision changes over the planning horizon because human drivers tend to maintain their current driving decisions for relatively long periods. In addition, we can rule out certain transitions that would not be considered by normal human drivers, such as the transition from $(\text{Gap1}, \text{LeftChange})$ to $(\text{Gap2}, \text{LeftChange})$.

2) *Actions of the Surrounding Vehicles*: Together with Assumptions 1 and 2, we make one additional working assumption for the SVs.

Assumption 3. *The surrounding vehicles keep their decisions unchanged throughout each forward simulation.*

Even though this assumption limits the decision space, it remains reasonable in practice since the behavior planner runs in a receding horizon fashion. In view of Assumptions 1 and 3, we define the action set of the VG as $\{\text{Assert}, \text{Yield}\}$. Assumption 2 indicates that the IV selects an action from the set $\Pi^{\text{VG}} := \{\text{Assert}, \text{Yield}\}$ while the other vehicles in the group adhere to car-following behavior. For instance, in Figure 2a, if the EV selects Gap1, then it mutually interacts with the SV1, and the SV2 just keeps a safety distance from the SV1.

B. Multi-vehicle Forward Simulation

1) *Vehicle Dynamics*: We generate the multi-vehicle trajectories by simulating the motion of the vehicles from the initial

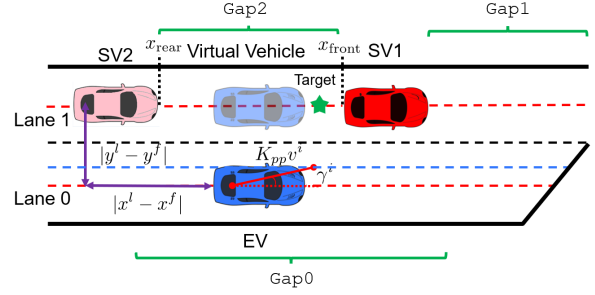


Fig. 3. Multi-vehicle forward simulation. $|x^l - x^f|$ and $|y^l - y^f|$ represent the longitudinal and lateral distances between the lane-changing vehicle (leader) and the interacting vehicle (follower), respectively.

states. We represent the dynamics of vehicle i as a kinematic bicycle:

$$\dot{p}_x^i = v^i \cos(\theta^i), \quad \dot{p}_y^i = v^i \sin(\theta^i), \quad \dot{\theta}^i = \frac{v^i}{l} \tan(\delta^i), \quad \dot{v}^i = a^i, \quad (3)$$

where (p_x^i, p_y^i) , θ^i and v^i are the position, the heading angle, and the speed, respectively; a^i and δ^i are the acceleration and the steering angle; l represents the inter-axle distance. The state and control input vectors are denoted as $x^i := (p_x^i, p_y^i, \theta^i, v^i)$ and $u^i := (a^i, \delta^i)$, respectively. We discretize the dynamics via the Runge-Kutta 3 method.

2) *Motion of the Ego Vehicle*: We apply two separate controllers to generate the longitudinal and lateral motion for the EV. For the longitudinal motion, we track the target longitudinal position and the desired speed using a PD controller [9]. One example of the target longitudinal position within the desired gap is illustrated in Figure 3. The desired gap is defined based on the positions of the front and rear vehicles, denoted as x_{front} and x_{rear} , respectively. Similarly to [9], [39], we determine the target longitudinal position and the desired speed using a rule-based method. The output of the PD controller is represented by a_{pd} . However, this controller does not consider the lead vehicle and the static obstacle. Hence, to avoid a collision, we obtain the car-following acceleration a_{idm} using the intelligent driver model (IDM) [42]. Overall, for the sake of safety, we select the minimum acceleration as the command, $a_{\text{cmd}} := \min(a_{\text{pd}}, a_{\text{idm}})$.

As for the lateral motion, we adopt a pure pursuit controller that uses the current vehicle speed and the target line as inputs. The steering angle is computed by $\delta_{\text{cmd}}^i = \tan^{-1}\left(\frac{2l \sin(\gamma^i)}{K_{pp} v^i}\right)$, where γ^i represents the angle between the heading direction and lookahead direction, K_{pp} is the feedback gain, and $K_{pp} v^i$ is the lookahead distance.

3) *Motion of the Surrounding Vehicles*: Our goal is to model the car-following behavior and the reaction to the lane-changing vehicle. The IDM is a common traffic model, but it focuses solely on the car following task, disregarding vehicles on adjacent lanes. Therefore, we propose a modified IDM, which considers lane-changing vehicles by projecting them onto their target lanes, resulting in virtual vehicles as shown in Figure 3. Subsequently, we calculate the distance between the

virtual leader and the follower using the following equation:

$$d_{\text{idm}} = |x^l - x^f| e^{\kappa|y^l - y^f|}, \quad \kappa = 2 \log(\beta) / w_{\text{lane}}, \quad (4)$$

where w_{lane} is the lane width, and β is a parameter characterizing the level of willingness to yield. By adjusting the value of β , we can model different actions performed by the VG. Specifically, a large value of β indicates that the vehicle on the target lane is less likely to yield to the lane-changing vehicle because it perceives that the projection is far away. When the lateral distance between two vehicles vanishes, that is $|y^l - y^f| = 0$, the virtual distance between them is equivalent to the actual longitudinal distance.

C. Trajectory Evaluation

1) *Cost Function*: After generating multi-vehicle trajectories, we proceed to select a specific action pair by solving a matrix game. For constructing the cost matrix, we first introduce the cost function J^i of vehicle i , which is typically a combination of several user-defined metrics, including safety, efficiency, comfort, navigation, and information cost: $J^i = J_{\text{saf}}^i + J_{\text{eff}}^i + J_{\text{com}}^i + J_{\text{nav}}^i + J_{\text{inf}}^i$. The value of the cost function J^i depends on the simulated trajectories, which are influenced by the semantic-level action of the EV, π^{EV} , and the VG, π^{VG} .

We calculate the safety cost by examining vehicle collisions. The footprint of vehicle i is modeled as a rectangle. If the distance between two rectangles is less than some small value, indicating a potential collision, we assign a huge penalty to the corresponding trajectory. Furthermore, we consider a dilated rectangle for each vehicle to encourage the vehicle to keep a suitable distance from the SVs. Next, we measure the efficiency of the trajectory by computing the difference between the vehicle speed and its desired speed. For the comfort cost, we consider the change in acceleration, which is known as jerk. Furthermore, we penalize the difference between the vehicle lateral position and its desired lateral position to encourage the lane-changing maneuver. Additionally, we introduce an information gain metric in the cost function, inspired by [43, Section 6], to motivate the EV to actively identify the intentions of the SVs. The reader can refer to our previous work [23] for more details on cost functions.

2) *Belief Update*: The EV needs to estimate the cost functions of the SVs by observing their trajectories since direct access to these cost functions is impossible in practice. Inspired by POMDP, we account for uncertainty in the aggregate cost of the SVs by integrating the beliefs into the cost function. The modified aggregate cost is computed as follows:

$$\bar{J}_{ij}^{\text{VG}} := (1 - b(\pi_i^{\text{VG}})) J_{ij}^{\text{VG}}, \quad \sum_{i=1}^{M^{\text{VG}}} b(\pi_i^{\text{VG}}) = 1,$$

where i and j represent the indices in the cost matrix, $\pi_i^{\text{VG}} \in \Pi^{\text{VG}}$ is the action of the VG, $M^{\text{VG}} := |\Pi^{\text{VG}}|$ denotes the cardinality of the action set of the VG, and b represents the belief about the action of the VG. This design can be understood as incorporating prior knowledge about the behavior of the VG into the aggregate cost. For example, if we have prior knowledge suggesting that the VG is inclined

to yield, then we can set the corresponding belief close to 1, which reduces the modified aggregate cost.

The belief is recursively updated at the beginning of each planning cycle using Bayes filtering [44]. The update rule involves two key components: the transition model $\mathbb{P}(\pi^{\text{VG}} | \pi_{-}^{\text{VG}})$ and the observation model $\mathbb{P}(o | \pi^{\text{VG}})$, where the notation π_{-} is associated with the previous planning cycle, and o denotes the observation vector comprising the historical states of the SVs. Assuming that the interacting vehicle in the group does not change its action, the transition model can be significantly simplified. In the simplified model, $\mathbb{P}(\pi^{\text{VG}} = \pi_j^{\text{VG}} | \pi_i^{\text{VG}})$ is equal to 1 if i and j coincide, and for all other cases, $\mathbb{P}(\pi^{\text{VG}} = \pi_j^{\text{VG}} | \pi_i^{\text{VG}})$ is equal to 0.

Regarding the observation model, we use the vehicle dynamics (1) with additive Gaussian noise to predict the state of the IV in the group:

$$x_{t+1}^{\text{VG}} = f(x_t^{\text{VG}}, u_t^{\text{VG}}(x_t, \pi_t^{\text{VG}}, \pi_t^{\text{EV}})) + w, \quad w \sim \mathcal{N}(0, W),$$

where $u_t^{\text{VG}}(\cdot)$ denotes the control policy discussed in Section IV-B3 and $w \sim \mathcal{N}(0, W)$ is additive Gaussian noise with zero mean and covariance matrix W . Keeping this in mind, we can compute the likelihood of receiving an observation o using the following distribution:

$$\mathbb{P}(o | \pi^{\text{VG}}) \sim \mathcal{N}(f(x_{-}^{\text{VG}}, u_{-}^{\text{VG}}(x_{-}, \pi_{-}^{\text{VG}}, \pi_{-}^{\text{EV}})), W),$$

where the mean is the predicted state. With the transition model and the observation model, the belief update rule can be expressed as follows:

$$b(\pi^{\text{VG}}) = \frac{\mathbb{P}(o | \pi^{\text{VG}}) \sum_{\pi_{-}^{\text{VG}}} \mathbb{P}(\pi^{\text{VG}} | \pi_{-}^{\text{VG}}) b(\pi_{-}^{\text{VG}})}{\sum_{\pi_{-}^{\text{VG}}} \mathbb{P}(o | \pi_{-}^{\text{VG}}) \sum_{\pi^{\text{VG}}} \mathbb{P}(\pi^{\text{VG}} | \pi_{-}^{\text{VG}}) b(\pi_{-}^{\text{VG}})}.$$

3) *Equilibrium Selection*: After obtaining the cost matrix, we compute the Nash equilibrium of the matrix game by enumerating all possible combinations of semantic-level actions. If multiple Nash equilibria exist, we select the equilibrium with the lowest social cost [45], defined as $C_{ij} := J_{ij}^{\text{EV}} + J_{ij}^{\text{VG}}$. If a pure-strategy Nash equilibrium does not exist, we choose the Stackelberg equilibrium [21], [35] with the EV as the follower as a backup solution.

V. BRANCH MODEL PREDICTIVE CONTROL

From the coarse trajectory provided by the behavior planner, the motion planner aims at generating a safe, comfortable, and dynamically feasible trajectory. We model the motion planning problem as a stochastic optimal control problem due to the unknown behavior modes of the surrounding vehicles. In this section, we first introduce the technical background and then the general formulation of the interaction-aware motion planning problem. Subsequently, we introduce some simplifications to rapidly compute an approximate solution.

A. Technical Background

1) *Dynamics*: For simplicity, we consider two vehicles in this section: the ego vehicle (EV) and one interacting vehicle (IV), with the states denoted as x^{EV} and x^{IV} , respectively. The

joint state is represented as $\mathbf{x} := (x^{\text{EV}}, x^{\text{IV}})$. We model the vehicle dynamics by a discrete-time kinematic bicycle, where $i \in \{\text{EV}, \text{IV}\}$, $x^i := (p_x^i, p_y^i, \theta^i, v^i)$ and $u^i := (a^i, \delta^i)$ as in (3).

2) *Behavior Model*: We model the interactive behavior of the IV via the feedback policy $\kappa : \mathbb{R}^n \times \Omega \rightarrow \mathbb{R}^m$, where Ω is a finite set in which each element corresponds to one behavior mode of the IV. The control input of the IV at time step t is determined by both the joint state \mathbf{x}_t and the behavior mode $\omega_t \in \Omega$, that is,

$$u_t^{\text{IV}} = \kappa(\mathbf{x}_t, \omega_t), \quad \omega_t \sim b_t := \mathbb{P}(\omega_t | O_t), \quad (5)$$

where b_t , known as the belief state, is the distribution of ω_t conditioned on the observation O_t . The observation is a collection of the observed joint states $O_t := [\mathbf{x}_t, \mathbf{x}_{t-1}, \dots, \mathbf{x}_0]$. Similarly to [20], the EV updates the belief state based on Bayes filtering after obtaining a new observation. The belief update, also referred to as belief dynamics [15], can be briefly expressed as:

$$b_{t+1} = g(b_t, \mathbf{x}_{t+1}, u_t^{\text{EV}}).$$

In general, it is commonly believed that forward propagating the belief state analytically is intractable due to the nonlinear vehicle dynamics [13], [15]. Therefore, some approximations become necessary in practice, as shown in Section V-C.

B. General Formulation

With all the ingredients, we can now formulate the interaction-aware motion planning problem in the framework of stochastic optimal control:

$$\min_{(\mu_t^{\text{EV}})_{[0, T-1]}} \mathbb{E}_{\omega_t \sim b_t, t \in [0, T]} \left\{ \sum_{t=0}^{T-1} \ell(\mathbf{x}_t, u_t^{\text{EV}}) + \ell_f(\mathbf{x}_T) \right\} \quad (6a)$$

$$\text{s.t. } \mathbf{x}_0 = \bar{\mathbf{x}}, b_0 = \bar{b}, \quad (6b)$$

$$\forall t \in [0, T-1]:$$

$$x_{t+1}^{\text{EV}} = f(x_t^{\text{EV}}, u_t^{\text{EV}}), u_t^{\text{EV}} = \mu_t^{\text{EV}}(\mathbf{x}_t, b_t), \quad (6c)$$

$$x_{t+1}^{\text{IV}} = f(x_t^{\text{IV}}, u_t^{\text{IV}}), u_t^{\text{IV}} = \kappa(\mathbf{x}_t, \omega_t), \quad (6d)$$

$$b_{t+1} = g(b_t, \mathbf{x}_{t+1}, u_t^{\text{EV}}), \quad (6e)$$

$$u_t^{\text{EV}} \in \mathcal{U}, \quad (6f)$$

$$\forall t \in [0, T]: h(\mathbf{x}_t) \leq 0, \quad (6g)$$

where $(\mu_t^{\text{EV}})_{[0, T-1]}$ is a sequence of feedback control policies, $\bar{\mathbf{x}}$ and \bar{b} are the initial joint state and belief, $\mathcal{U} \subseteq \mathbb{R}^m$ is the set of feasible control inputs, and (6g) represents the collision avoidance constraints. An alternative to the hard collision avoidance constraints is a chance constraint formulation which ensures safety in a probabilistic manner and reduces conservatism at the price of higher computational effort [14], [16]. Thus, to achieve a balance between robustness and computational demands, we adopt soft collision avoidance constraints in practice [46] and in turn sacrifice strict probabilistic guarantees.

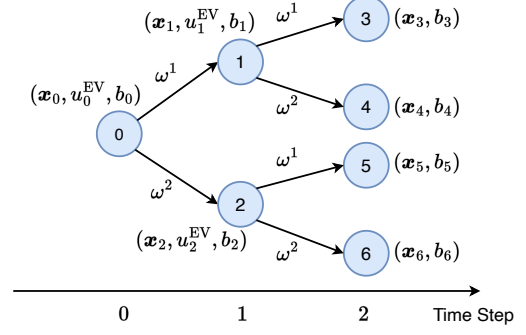


Fig. 4. Trajectory tree with a horizon of $T = 2$. The tree branches out at each time step based on the behavior mode $\omega_t \in \Omega := \{\omega^1, \omega^2\}$. A transition probability P_i pertains to each branch. In this example, $\mathcal{N} = \{0, 1, 2, 3, 4, 5, 6\}$ and $\mathcal{L} = \{3, 4, 5, 6\}$.

C. Trajectory Tree

Let us now present an approximation of the general interaction-aware motion planning problem. In a numerical optimal control problem, we often look for a sequence of control inputs $(u_t^{\text{EV}})_{[0, T-1]}$ rather than a sequence of feedback policies $(\mu_t^{\text{EV}})_{[0, T-1]}$ to reduce the computational complexity. Nevertheless, if we seek a sequence of control inputs solving (6), it might be overly conservative or even not exist in some cases due to the requirement that constraints must be respected across all realizations of uncertainty. Another primary drawback of this approximation is neglecting the advantages that can be gained from future observations. To resolve this, we instead seek a trajectory tree where all possible realizations of uncertainty are enumerated. As shown in Figure 4, the tree is rooted at the node of the current joint state and branches out at each time step based on the behavior mode. In contrast with a single control sequence, distinct control inputs at each predicted time step are derived based on different behavior modes. Using the trajectory tree, we reformulate the stochastic optimal control problem (6) as follows:

$$\min_{(u_i^{\text{EV}})_{i \in \mathcal{N} \setminus \mathcal{L}}} \sum_{i \in \mathcal{L}} P_i \ell_f(\mathbf{x}_i) + \sum_{i \in \mathcal{N} \setminus \mathcal{L}} P_i \ell(\mathbf{x}_i, u_i^{\text{EV}}) \quad (7a)$$

$$\text{s.t. } \mathbf{x}_0 = \bar{\mathbf{x}}, b_0 = \bar{b}, \quad (7b)$$

$$\forall i \in \mathcal{N} \setminus \{0\}: \quad (7c)$$

$$x_i^{\text{EV}} = f(x_{p(i)}^{\text{EV}}, u_{p(i)}^{\text{EV}}), \quad (7d)$$

$$x_i^{\text{IV}} = f(x_{p(i)}^{\text{IV}}, u_{p(i)}^{\text{IV}}), u_{p(i)}^{\text{IV}} = \kappa(\mathbf{x}_{p(i)}, \omega_{p(i)}), \quad (7e)$$

$$b_i = g(b_{p(i)}, \mathbf{x}_i, u_{p(i)}^{\text{EV}}), \quad (7f)$$

$$\forall i \in \mathcal{N} \setminus \mathcal{L}: u_i^{\text{EV}} \in \mathcal{U}, \quad (7g)$$

$$\forall i \in \mathcal{N}: h(\mathbf{x}_i) \leq 0, \quad (7h)$$

where \mathcal{N} and \mathcal{L} denote the set of all tree nodes and the set of all leaf nodes, respectively, $p(i)$ represents the parent node of node i , and P_i is the transition probability from a parent node $p(i)$ to its child node i .

While the trajectory tree in (7) is a reasonable approximation of a sequence of feedback policies, it still entails several practical challenges. First, the introduction of additional opti-

mization variables results in an increased computational burden. Furthermore, as the optimization problem is nonconvex, the quality of the computed solution is heavily dependent on the initial guess. Providing an initial trajectory tree is also a nontrivial task. Taking the aforementioned facts into account, we further simplify the trajectory tree as follows:

- (i) The trajectory tree only branches out once, which assumes that the behavior mode of the IV remains constant over the planning horizon and the EV is fully certain about the behavior mode of the IV after the first branch. As a result, we do not consider the belief update in (7f) over the planning horizon. Additionally, our behavior planner can easily initialize such a simplified tree, enhancing the quality of the computed solution.
- (ii) The behavior planner provides the multi-modal state trajectories of the IV, which can be viewed as an open-loop control policy. Compared with using feedback control policy in (5), we ignore the mutual interaction in motion planning since it has been taken into account by the behavior planner.

We note that the simplified tree shares some similarities with those found in QMDP [44] and contingency planning [12], [47]. Figure 5 shows an example of the simplified trajectory tree with two branches. We now can discuss the formulation in more detail.

D. Detailed Formulation

1) *Branches*: In a Nash game, all vehicles are treated equally [18]. However, this game structure does not always hold in practice; thus, a Nash game might fail to capture the actual interaction between vehicles. In such cases, it becomes necessary to consider other interaction models. One alternative candidate is a Stackelberg game with a leader-follower structure [21], [35]. In our design, we utilize the trajectory tree to combine the two interaction models. Specifically, all the vehicles play their Nash strategies in the nominal branch while the Stackelberg equilibrium is followed in the backup branch.

2) *Cost function*: The motion planner intends to track the reference trajectories generated by the behavior planner while maximizing the level of comfort. Thus, we use the following stage cost:

$$\begin{aligned} \ell &:= \ell_{\text{track}} + \ell_{\text{com}}, \\ \ell_{\text{track}}(x_i^{\text{EV}}, u_i^{\text{EV}}) &:= \left\| x_i^{\text{EV}} - x_i^{\text{EV, ref}} \right\|_Q^2 + \left\| u_i^{\text{EV}} - u_i^{\text{EV, ref}} \right\|_R^2, \\ \ell_{\text{com}}(u_i^{\text{EV}}, u_{p(i)}^{\text{EV}}) &:= \left\| u_i^{\text{EV}} - u_{p(i)}^{\text{EV}} \right\|_{R_{\text{com}}}^2, \quad \forall i \in \mathcal{N}, \end{aligned}$$

where $R_{\text{com}} \succ 0$, $Q \succ 0$, and $R \succ 0$ represent weight matrices for comfort, state, and control input, respectively; we define $u_{p(0)}^{\text{EV}}$ as the executed control command from the last planning cycle. The penalty term on the change rate of the control input plays an important role in enhancing the comfort of the generated trajectories. By penalizing $\left\| u_0^{\text{EV}} - u_{p(0)}^{\text{EV}} \right\|_{R_{\text{com}}}^2$, we reduce the executed control variation between two planning cycles.

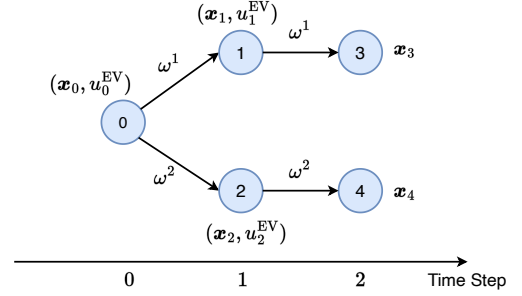


Fig. 5. Simplified trajectory tree. The tree has multiple branches exclusively at the root node, while all other nodes, except for the leaf nodes, have only one single branch.

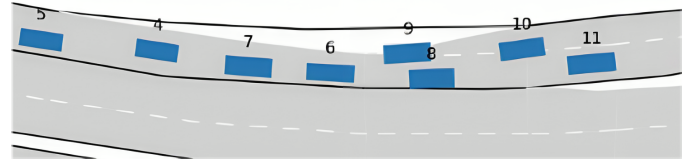


Fig. 6. On-ramp merging scenario: vehicle 9 intends to reach the gap between vehicles 6 and 8. Since the gap is not sufficiently large, vehicle 9 has to identify the intention of vehicle 8 and make an appropriate decision.

3) *State and input constraints*: We impose lower and upper bounds on the state and control input to ensure physical feasibility:

$$x_{\text{lb}} \leq x_i^{\text{EV}} \leq x_{\text{ub}}, \quad \forall i \in \mathcal{N}, \quad u_{\text{lb}} \leq u_i^{\text{EV}} \leq u_{\text{ub}}, \quad \forall i \in \mathcal{N} \setminus \mathcal{L}.$$

4) *Collision avoidance*: The footprint of a vehicle can be naturally represented by a rectangle. Nevertheless, one challenge associated with this representation is the complexity of deriving a closed-form signed distance. Moreover, the gradient of the signed distance function is discontinuous, which poses a challenge to the optimization solver. To circumvent these difficulties, we model the footprint of a vehicle as a series of linked discs [14], and formulate the smooth collision avoidance constraints as follows:

$$\begin{aligned} (r^{\text{EV}} + r^{\text{IV}})^2 - \|c_i(x^{\text{EV}}) - c_j(x^{\text{IV}})\|_2^2 &\leq 0, \\ i \in [1, n_c^{\text{EV}}], \quad j \in [1, n_c^{\text{IV}}], \end{aligned}$$

where r^{EV} and r^{IV} represent the disc radii, $c: \mathbb{R}^n \rightarrow \mathbb{R}^2$ is a function that computes the center of the disc, and n_c^{EV} , n_c^{IV} denote the number of discs used for approximating the vehicle footprints.

VI. NUMERICAL SIMULATIONS

A. Benchmarking

We validate our proposed game-theoretic planner using the INTERACTION dataset [24]. We consider the on-ramp merging scenario shown in Figure 6, where the ego vehicle must complete the lane change before reaching the end of the current lane. Considering various factors, such as traffic speeds, vehicle sizes, and behavior modes, we select 100 tracks from the dataset and mark the ego vehicle for each track. Each

track has a duration of $T_{tr} = 4$ s with a discretization step of $\Delta t = 100$ ms, and the number of timestamps is $N_{ts} = T_{tr}/\Delta t$. We control the ego vehicle via our proposed planner, while the motion of the surrounding vehicles is simulated by replaying the trajectory data. We compare the proposed GTBP-BMPC with three baseline methods:

- ABP-MPC, which comprises an ordinary behavior planner and a traditional MPC motion planner. The behavior planner assumes that the decision of the vehicle group is always `Assert`. The traditional motion planner outputs a sequence of control inputs rather than a trajectory tree.
- YBP-MPC, which differs from ABP-MPC in assuming that the vehicle group `yields` to the ego vehicle.
- GTBP-MPC [23], which includes a game-theoretic behavior planner and a traditional MPC motion planner. This method only considers multi-modal behavior at the behavior planning level.

We evaluate the quality of the trajectories by examining metrics related to safety, progress, comfort, and displacement errors as follows:

- We assess the safety level via collision rate and Time-to-Collision (TTC) [37]. The collision rate is defined as the proportion of the number of cases, in which a collision happens, to the total number of cases. TTC refers to the time it takes for two vehicles to collide if they maintain their current speed and heading. For each pair of trajectories, we compute TTC_k at timestamp k and select the minimum of $\{TTC_k\}$ as TTC_{traj} .
- To evaluate progress, we compute the longitudinal and lateral distances by projecting the vehicle position at the final timestamp onto the target lane.
- We employ the root mean squared acceleration, maximum absolute acceleration, and root mean squared angular acceleration as metrics to measure the level of comfort [48], [49].
- We use average displacement error (ADE) to measure the distance between the generated trajectory and the ground truth [9]. Specifically, $ADE := \sum_{k=1}^{N_{ts}} \|p_k^{EV} - p_k^{EV, GT}\| / N_{ts}$, where $p_k^{EV, GT}$ denotes the ground truth position of the ego vehicle at timestamp k .

B. Implementation details

1) *Game-theoretic behavior planner*: We use a planning horizon of $T_{bp} = 25$, a discretization step of $\Delta t_{bp} = 0.2$ s, a decision time period of $\Delta h = 1$ s and a decision horizon of $H = 5$. In other words, the behavior planner looks ahead for 5 s and makes a semantic-level decision every 1 s. We run the behavior planner at 5 Hz in a receding horizon fashion.

We select the vehicle nearest to the ego vehicle as the target vehicle (SV1). The vehicles ahead of and behind the target vehicle are denoted as SV0 and SV2, respectively. The gap in front of the target vehicle is denoted as Gap_1 , while the gap behind is referred to as Gap_2 , as illustrated in Figure 2a. We label the current lane where the ego vehicle stays as Gap_0 . As mentioned in Section IV-A, there are three desired lateral positions: two center lines and one probing line.

TABLE I
STATISTICAL RESULTS

Metric	GTBP-BMPC	GTBP-MP	ABP-MP	YBP-MP
collision rate (%)	0	0	1	1
longitudinal progress (m)	9.68	9.73	9.84	9.61
lateral progress (m)	1.22	1.19	1.34	1.11
RMS abs acc. (m/s ²)	0.37	0.38	0.41	0.38
max abs acc. (m/s ²)	0.54	0.54	0.60	0.55
RMS heading acc. (rad/s ²)	0.14	0.15	0.12	0.13
ADE (m)	0.69	0.69	0.77	0.72

The surrounding vehicles, SV0, SV1, and SV2 are considered as a vehicle group. The potential interacting vehicles in this group are the SV1 and SV2. We assume that the interacting vehicle has two longitudinal actions: `Assert` and `Yield`. Each action corresponds to one driving behavior of the interacting vehicle. To represent the two actions, we supply distinct parameters to the modified IDM, which controls the motion of the surrounding vehicle. For instance, to model a yielding vehicle, in addition to the willingness indicator β in (4), we set the minimum spacing and desired time headway to relatively large values.

2) *BMPC*: The motion planner operates at 10 Hz with a discretization step of 0.1 s and a planning horizon of 4 s. The reference trajectories for the ego vehicle come from the output of the behavior planner. The probability associated with the tree branch is also provided by the behavior planner. To exploit the sparse structure of the optimal control problem, we develop a tailored BMPC solver by extending the iLQR-based solver [50] to the trajectory tree version known as iLQR-tree solver [30], [48]. We handle state and control input constraints using the augmented Lagrangian relaxation [51].

All simulations are conducted on a laptop with a 2.30 GHz Intel Core i7-11800H processor and 16 GB RAM. The average computation time for the BMPC problem is 1.11 ms, while the peak computation time reaches 7.23 ms. We further enhance the computational efficiency by computing the backward sweeps from each leaf node to the shared node in parallel via OpenMP API. As a result, we achieve a reduction of 9.9% in the mean computation time (1.00 ms) and a decrease of 19.2% in the maximum computation time (5.84 ms).

C. Statistical results

We compare the proposed planner with three baseline planners across 100 test scenarios. Table I shows the mean values of the considered metrics for these scenarios.

1) *Safety*: The game-theoretic planners generate safe closed-loop trajectories across all test scenarios, whereas the others do not. As YBP-MPC assumes the interacting vehicle behaves politely, a collision is prone to occur when the interacting vehicle fails to yield. We compute TTC_{traj} to evaluate the safety level further, and the statistical results are illustrated in Figure 7a. The mean and lower quartile of GTBP-BMPC exceed those of GTBP-MPC, indicating that GTBP-

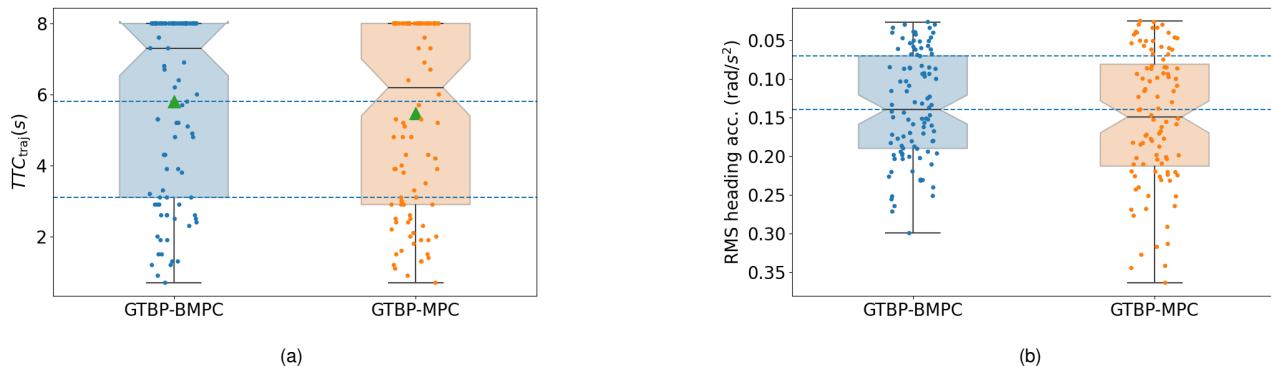


Fig. 7. (a): Box plot of TTC_{traj} . For visualization, we limit TTC_{traj} to 8 s. The triangle marker represents the mean value. (b): Box plot of root mean squared heading acceleration.

BMPC generates trajectories with a larger safety margin across the majority of test scenarios.

2) *Progress*: ABP-MPC achieves the largest longitudinal progress, but its lateral progress is the worst. Consequently, the ego vehicle controlled by ABP-MPC has a risk of missing the lane-merging opportunity. In contrast, YBP-MPC performs worst in longitudinal progress but excels in lateral progress. Compared to ABP-MPC and YBP-MPC, the game-theoretic planners, GTBP-BMPC and GTBP-MPC, strike the best balance between longitudinal and lateral progress.

3) *Comfort*: Regarding comfort assessment, all the planners, except for ABP-MPC, achieve comparable performance. Figure 7b illustrates that GTBP-BMPC outperforms GTBP-MPC with respect to heading acceleration. This improvement is attributed to the ability of the trajectory tree to mitigate the issue arising from abrupt changes in semantic-level actions between two planning cycles.

4) *Comparison with ground-truth trajectories*: The lowest ADE value of the trajectories obtained by GTBP-BMPC indicates that the ego vehicle controlled by GTBP-BMPC exhibits more human-like driving behavior.

Overall, the key takeaway is the significance of incorporating multiple behavior modes. ABP-MPC and YBP-MPC fail to handle the mismatch between the considered and actual behavior modes, which may lead to lane change failure or even collision.

TABLE II
CASE STUDY

Metric	GTBP-BMPC	GTBP-MP	YBP-MP
collision-free	✓	✓	✗
TTC_{traj} (s)	2.90	1.10	
longitudinal progress (m)	7.45	7.32	
RMS abs acc. (m/s^2)	0.44	0.41	
max abs acc. (m/s^2)	0.53	0.53	
RMS heading acc. (rad/s^2)	0.16	0.33	

D. Case study

We choose one interesting scenario to illustrate the effectiveness of the integration of the game-theoretic behavior planner and the BMPC framework. The key frames of the simulation are illustrated in Figure 8. The ego vehicle (vehicle 9) faces two major challenges in this scenario. First, the feasible driving space is limited due to the narrow environment. Secondly, the actual behavior mode of vehicle 10 is variable. Specifically, vehicle 10 decelerates during the initial 1 s but speeds up afterward. Consequently, all the ego vehicles in Figure 8 decide to change the lane in the beginning but finally cancel the lane change. In Figure 8c, as the ego vehicle does not realize that merging is dangerous in time, a collision with vehicle 10 becomes unavoidable. On the contrary, the closed-loop trajectories generated by GTBP-BMPC and GTBP-MPC are collision-free thanks to the consideration of multi-modal behavior. We observe that the distance between the ego vehicle and vehicle 10 at 3.5 s in Figure 8a is larger than that in Figure 8b, and the corresponding TTC_{traj} values in Table II further affirm that GTBP-BMPC outputs a safer trajectory, as it allows the ego vehicle to safely return to the original lane by adhering to the backup plan. Furthermore, GTBP-BMPC outperforms GTBP-MPC in terms of longitudinal progress and RMS heading acceleration.

VII. CONCLUSION

In this paper, we present a game-theoretic planning framework to address lane-merging problems in interactive environments. Our approach explicitly models the interaction between vehicles using a matrix game and tackles the issue caused by the uncertain behavior of the surrounding vehicles via BMPC. By using multi-vehicle trajectories outputted by the behavior planner as an initial guess, we prevent the BMPC planner from getting stuck in an undesirable local solution. Our validation study on the INTERACTION dataset indicates the necessity of interaction modeling and demonstrates the superior performance of our proposed method compared to the state-of-the-art approaches. We believe that the proposed planning framework provides a promising direction for developing more efficient and interactive autonomous driving systems.

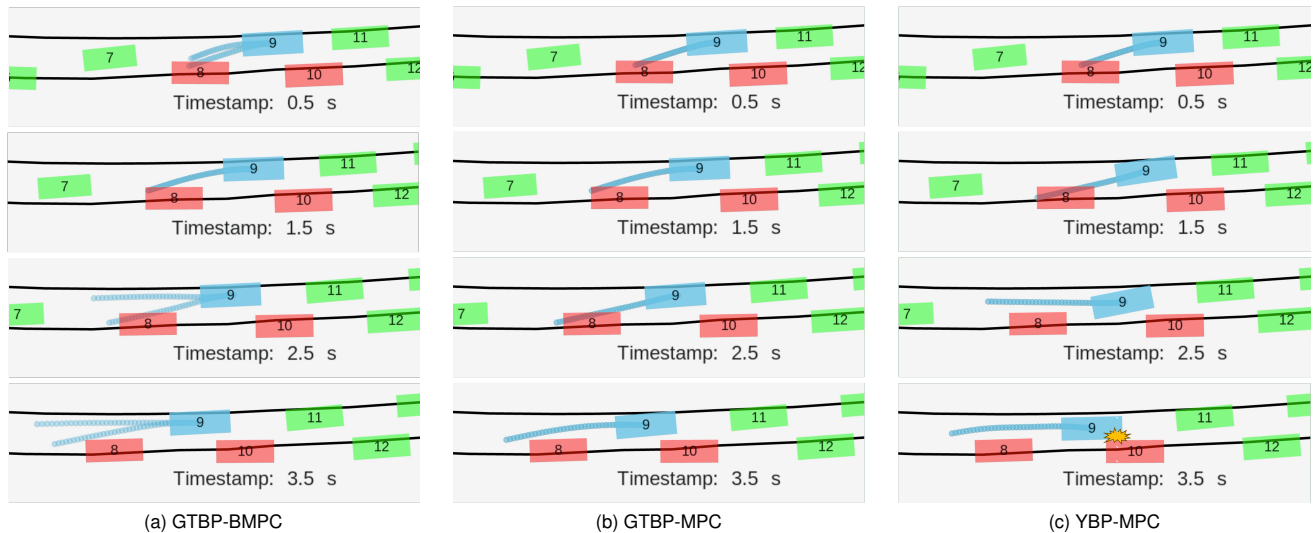


Fig. 8. Key frames of the selected scenario. The ego vehicle is highlighted in blue, while the potential interacting vehicles are marked in red. The ego vehicles in (a)-(c) are controlled by GTBP-BMPC, GTBP-MPC, and YBP-MPC, respectively.

In future work, we plan to further improve the computational efficiency and robustness of the BMPC planner. In addition, we intend to extend this planning framework to accommodate intersection-crossing scenarios. Furthermore, we will implement the behavior planner in C++ and validate the whole planning framework on a hardware platform.

REFERENCES

- [1] W. Ding, L. Zhang, J. Chen, and S. Shen, "Safe Trajectory Generation for Complex Urban Environments Using Spatio-Temporal Semantic Corridor," *IEEE Robotics and Automation Letters*, vol. 4, no. 3, pp. 2997–3004, Jul. 2019.
- [2] H. Fan, F. Zhu, C. Liu, *et al.*, "Baidu Apollo EM Motion Planner," *arXiv:1807.08048 [cs]*, Jul. 2018, arXiv: 1807.08048.
- [3] W. Zeng, W. Luo, S. Suo, *et al.*, "End-To-End Interpretable Neural Motion Planner," in *2019 IEEE/CVF Conference on Computer Vision and Pattern Recognition (CVPR)*, Long Beach, CA, USA: IEEE, Jun. 2019, pp. 8652–8661.
- [4] D. Chen and P. Krahenbuhl, "Learning from All Vehicles," in *2022 IEEE/CVF Conference on Computer Vision and Pattern Recognition (CVPR)*, New Orleans, LA, USA: IEEE, Jun. 2022, pp. 17201–17210.
- [5] M. Lauri, D. Hsu, and J. Pajarinen, "Partially Observable Markov Decision Processes in Robotics: A Survey," *IEEE Transactions on Robotics*, vol. 39, no. 1, pp. 21–40, Feb. 2023.
- [6] C. Hubmann, J. Schulz, G. Xu, D. Althoff, and C. Stiller, "A Belief State Planner for Interactive Merge Maneuvers in Congested Traffic," in *2018 21st International Conference on Intelligent Transportation Systems (ITSC)*, Nov. 2018, pp. 1617–1624.
- [7] C. Hubmann, J. Schulz, M. Becker, D. Althoff, and C. Stiller, "Automated driving in uncertain environments: Planning with interaction and uncertain maneuver prediction," *IEEE Transactions on Intelligent Vehicles*, vol. 3, no. 1, pp. 5–17, 2018.
- [8] A. G. Cunningham, E. Galceran, R. M. Eustice, and E. Olson, "MPDM: Multipolicy decision-making in dynamic, uncertain environments for autonomous driving," in *2015 IEEE International Conference on Robotics and Automation (ICRA)*, Seattle, WA, USA: IEEE, May 2015, pp. 1670–1677.
- [9] W. Ding, L. Zhang, J. Chen, and S. Shen, "EPSILON: An Efficient Planning System for Automated Vehicles in Highly Interactive Environments," *IEEE Transactions on Robotics*, vol. 38, no. 2, pp. 1118–1138, Apr. 2022.
- [10] M. J. Kochenderfer, *Decision making under uncertainty: theory and application*. MIT press, 2015.
- [11] Y. Chen, U. Rosolia, W. Ubellacker, N. Csomay-Shanklin, and A. D. Ames, "Interactive multi-modal motion planning with branch model predictive control," *IEEE Robotics and Automation Letters*, vol. 7, no. 2, pp. 5365–5372, 2022.
- [12] J. Hardy and M. Campbell, "Contingency planning over probabilistic obstacle predictions for autonomous road vehicles," *IEEE Transactions on Robotics*, vol. 29, no. 4, pp. 913–929, 2013.
- [13] D. Qiu, Y. Zhao, and C. Baker, "Latent Belief Space Motion Planning under Cost, Dynamics, and Intent Uncertainty," in *Robotics: Science and Systems XVI*, Robotics: Science and Systems Foundation, Jul. 2020, ISBN: 978-0-9923747-6-1.
- [14] R. Wang, M. Schuurmans, and P. Patrinos, "Interaction-aware model predictive control for autonomous driving," in *2023 European Control Conference (ECC)*, 2023, pp. 1–6.
- [15] H. Hu and J. F. Fisac, "Active Uncertainty Reduction for Human-Robot Interaction: An Implicit Dual Control Approach," in *Algorithmic Foundations of Robotics XV*, S. M. LaValle, J. M. O’Kane, M. Otte, D. Sadigh, and P. Tokekar, Eds., ser. Springer Proceedings in Advanced Robotics, Cham: Springer International Publishing, 2023, pp. 385–401, ISBN: 978-3-031-21090-7.
- [16] H. Ahn, C. Chen, I. M. Mitchell, and M. Kamgarpour, "Safe motion planning against multimodal distributions based on a scenario approach," *IEEE Control Systems Letters*, vol. 6, pp. 1142–1147, 2022.
- [17] A. Wang, A. Jasour, and B. C. Williams, "Non-gaussian chance-constrained trajectory planning for autonomous vehicles under agent uncertainty," *IEEE Robotics and Automation Letters*, vol. 5, no. 4, pp. 6041–6048, 2020.
- [18] S. L. Cleac’h, M. Schwager, and Z. Manchester, "ALGAMES: A Fast Solver for Constrained Dynamic Games," in *Robotics: Science and Systems XVI*, Jul. 2020. arXiv: 1910.09713 [cs].
- [19] X. Liu, L. Peters, and J. Alonso-Mora, *Learning to play trajectory games against opponents with unknown objectives*, 2023.
- [20] K. Liu, N. Li, H. E. Tseng, I. Kolmanovsky, and A. Girard, "Interaction-Aware Trajectory Prediction and Planning for Autonomous Vehicles in Forced Merge Scenarios," *IEEE Transactions on Intelligent Transportation Systems*, vol. 24, no. 1, pp. 474–488, Jan. 2023.
- [21] C. Wei, Y. He, H. Tian, and Y. Lv, "Game Theoretic Merging Behavior Control for Autonomous Vehicle at Highway On-Ramp," *IEEE Transactions on Intelligent Transportation Systems*, vol. 23, no. 11, pp. 21127–21136, Nov. 2022.
- [22] V. G. Lopez, F. L. Lewis, M. Liu, Y. Wan, S. Nagesh Rao, and D. Filev, "Game-Theoretic Lane-Changing Decision Making and Payoff Learning for Autonomous Vehicles," *IEEE Transactions on Vehicular Technology*, vol. 71, no. 4, pp. 3609–3620, Apr. 2022.
- [23] L. Zhang, S. Han, and S. Grammatico, "An efficient game-theoretic planner for automated lane merging with multi-modal behavior under-

- standing,” in *2023 IEEE 26th International Conference on Intelligent Transportation Systems (ITSC)*, Sep. 2023.
- [24] W. Zhan, L. Sun, D. Wang, *et al.*, “INTERACTION Dataset: An INTERnational, Adversarial and Cooperative motION Dataset in Interactive Driving Scenarios with Semantic Maps,” *arXiv:1910.03088 [cs, eess]*, Sep. 2019.
- [25] D. Silver and J. Veness, “Monte-Carlo Planning in Large POMDPs,” in *Advances in Neural Information Processing Systems*, vol. 23, Curran Associates, Inc., 2010.
- [26] Z. Sunberg and M. J. Kochenderfer, “Improving Automated Driving Through POMDP Planning With Human Internal States,” *IEEE Transactions on Intelligent Transportation Systems*, vol. 23, no. 11, pp. 20073–20083, Nov. 2022.
- [27] P. Cai, Y. Luo, D. Hsu, and W. S. Lee, “HyP-DESPOt: A hybrid parallel algorithm for online planning under uncertainty,” *The International Journal of Robotics Research*, vol. 40, no. 2-3, pp. 558–573, Feb. 2021.
- [28] J. Fischer, E. Bührle, D. Kamran, and C. Stiller, “Guiding Belief Space Planning with Learned Models for Interactive Merging,” in *2022 IEEE 25th International Conference on Intelligent Transportation Systems (ITSC)*, Oct. 2022, pp. 2542–2549.
- [29] B. Zhou, W. Schwarting, D. Rus, and J. Alonso-Mora, “Joint multi-policy behavior estimation and receding-horizon trajectory planning for automated urban driving,” in *2018 IEEE International Conference on Robotics and Automation (ICRA)*, 2018, pp. 2388–2394.
- [30] F. Da, “Comprehensive reactive safety: No need for a trajectory if you have a strategy,” in *2022 IEEE/RSJ International Conference on Intelligent Robots and Systems (IROS)*, 2022, pp. 2903–2910.
- [31] I. Batkovic, U. Rosolia, M. Zanon, and P. Falcone, “A robust scenario mpc approach for uncertain multi-modal obstacles,” *IEEE Control Systems Letters*, vol. 5, no. 3, pp. 947–952, 2021.
- [32] D. Fridovich-Keil, E. Ratner, L. Peters, A. D. Dragan, and C. J. Tomlin, “Efficient iterative linear-quadratic approximations for non-linear multi-player general-sum differential games,” in *2020 IEEE International Conference on Robotics and Automation (ICRA)*, 2020, pp. 1475–1481.
- [33] W. Schwarting, A. Pierson, J. Alonso-Mora, S. Karaman, and D. Rus, “Social behavior for autonomous vehicles,” *Proceedings of the National Academy of Sciences*, vol. 116, no. 50, pp. 24972–24978, 2019. eprint: <https://www.pnas.org/doi/pdf/10.1073/pnas.1820676116>.
- [34] L. Peters, V. Rubies-Royo, C. J. Tomlin, *et al.*, “Online and offline learning of player objectives from partial observations in dynamic games,” *The International Journal of Robotics Research*, vol. 42, no. 10, pp. 917–937, 2023.
- [35] Q. Zhang, R. Langari, H. E. Tseng, D. Filev, S. Szwabowski, and S. Coskun, “A game theoretic model predictive controller with aggressiveness estimation for mandatory lane change,” *IEEE Transactions on Intelligent Vehicles*, vol. 5, no. 1, pp. 75–89, 2020.
- [36] R. Tian, L. Sun, M. Tomizuka, and D. Isele, “Anytime Game-Theoretic Planning with Active Reasoning About Humans’ Latent States for Human-Centered Robots,” in *2021 IEEE International Conference on Robotics and Automation (ICRA)*, May 2021, pp. 4509–4515.
- [37] D. Li, H. Pan, Y. Xiao, *et al.*, “Social-aware decision algorithm for on-ramp merging based on level-k gaming,” in *2022 IEEE 18th International Conference on Automation Science and Engineering (CASE)*, 2022, pp. 1753–1758.
- [38] K. Ji, N. Li, M. Orsag, and K. Han, “Hierarchical and game-theoretic decision-making for connected and automated vehicles in overtaking scenarios,” *Transportation Research Part C: Emerging Technologies*, vol. 150, p. 104 109, May 2023.
- [39] S. Shalev-Shwartz, S. Shammah, and A. Shashua, *On a Formal Model of Safe and Scalable Self-driving Cars*, arXiv:1708.06374 [cs, stat], Oct. 2018.
- [40] T. Başar and G. J. Olsder, *Dynamic Noncooperative Game Theory, 2nd Edition*. Society for Industrial and Applied Mathematics, Jan. 1998.
- [41] W. Wang, L. Wang, C. Zhang, C. Liu, and L. Sun, “Social Interactions for Autonomous Driving: A Review and Perspectives,” *Foundations and Trends® in Robotics*, vol. 10, no. 3-4, pp. 198–376, 2022.
- [42] M. Treiber, A. Hennecke, and D. Helbing, “Congested Traffic States in Empirical Observations and Microscopic Simulations,” *Physical Review E*, vol. 62, no. 2, pp. 1805–1824, Aug. 2000, arXiv:cond-mat/0002177.
- [43] D. Sadigh, N. Landolfi, S. S. Sastry, S. A. Seshia, and A. D. Dragan, “Planning for cars that coordinate with people: Leveraging effects on human actions for planning and active information gathering over human internal state,” *Autonomous Robots*, vol. 42, no. 7, pp. 1405–1426, Oct. 2018.
- [44] S. Thrun, “Probabilistic robotics,” *Communications of the ACM*, vol. 45, no. 3, pp. 52–57, Mar. 2002.
- [45] A. Zanardi, E. Mion, M. Bruschetta, S. Bolognani, A. Censi, and E. Frazzoli, “Urban Driving Games With Lexicographic Preferences and Socially Efficient Nash Equilibria,” *IEEE Robotics and Automation Letters*, vol. 6, no. 3, pp. 4978–4985, Jul. 2021.
- [46] A. Liniger, A. Domahidi, and M. Morari, “Optimization-Based Autonomous Racing of 1:43 Scale RC Cars,” *Optimal Control Applications and Methods*, vol. 36, no. 5, pp. 628–647, Sep. 2015, arXiv:1711.07300 [cs, math].
- [47] J. P. Alsterda, M. Brown, and J. C. Gerdes, “Contingency model predictive control for automated vehicles,” in *2019 American Control Conference (ACC)*, 2019, pp. 717–722.
- [48] T. Li, L. Zhang, S. Liu, and S. Shen, “Marc: Multipolicy and risk-aware contingency planning for autonomous driving,” *IEEE Robotics and Automation Letters*, vol. 8, no. 10, pp. 6587–6594, 2023.
- [49] S. Bae, D. Isele, A. Nakhaei, *et al.*, “Lane-change in dense traffic with model predictive control and neural networks,” *IEEE Transactions on Control Systems Technology*, vol. 31, no. 2, pp. 646–659, 2023.
- [50] Y. Tassa, T. Erez, and E. Todorov, “Synthesis and stabilization of complex behaviors through online trajectory optimization,” in *2012 IEEE/RSJ International Conference on Intelligent Robots and Systems*, 2012, pp. 4906–4913.
- [51] T. A. Howell, B. E. Jackson, and Z. Manchester, “Altro: A fast solver for constrained trajectory optimization,” in *2019 IEEE/RSJ International Conference on Intelligent Robots and Systems (IROS)*, 2019, pp. 7674–7679.